JET–R(98)03

# Lines of Sight for ITER Bolometers

L C Ingesson, R Reichle[1].

JET Joint Undertaking, Abingdon, Oxfordshire, OX14 3EA,

[1]Present address: CEA Cadarache, 13108 Saint-Paul-lez-Durance, France.

March 1998

## ABSTRACT

A proposal for lines of sight for bolometry on ITER is presented. Background of tomography relevant for the proposed system is discussed, in particular the complications of the coverage of projection space due to the non-convex shape of the inner wall of ITER. The requirements and technical constraints that led to the proposed system are discussed in detail. Simulations have been carried out to assess the performance of the system for emission profiles that are expected in ITER. The simulations are compared with simulations of systems with different numbers of lines of sight. Present tomography methods can make reasonable reconstructions of the divertor radiation from the measurements of about 400 lines of sight. The quality of the reconstructions decreases when fewer lines of sight are used; in particular, some features cannot be reconstructed well if a whole range of lines of sight is not used. The total emitted power is matched very well (within one percent), even with a reduced number of lines of sight. With the proposed number of lines of sight there is sufficient scope for improvement of the reconstructions of divertor radiation, bulk radiation, and in the presence of neutral particle effects on divertor bolometers.

## 1. INTRODUCTION

For ITER a bolometer system with high spatial resolution is foreseen. Recently, the latest design considerations have been reviewed [1]. The present document serves as a complement to this review by going into more detail on the selection criteria for lines of sight and on the phantom simulations that have been carried out to assess the capabilities of the proposed lay-out.

Bolometers are indispensable diagnostic instruments for ITER. They allow to control the radiated power fraction and the position and quantity of the radiation in the divertor, which is important for limiting the heat load onto divertor tiles. Furthermore, simulations of radiation profiles can be compared with measured profiles in order to assess the applicability of the models used in the simulations. An independent estimate of the emission profile requires full tomographic reconstructions without relying too much on restrictions given by models. The most demanding requirements are for full tomography, other quantities such as the total emitted power require only a subset of the channels. Therefore, the requirements for full tomography are assessed in the following. When a number of lines of sight (of the order of 400) are adequately chosen with varying coarseness for different regions, it seems to be possible to reconstruct the bulk radiation and in reasonable detail features in the divertor (10–20 cm).

The lay-out of ITER used in this report is based on the CATIA model of July 1997. It should be said that some of the features of the proposed bolometer lines of sight depend significantly on some design features of ITER that have changed regularly in designs (for example the blanket modules and shear keys). A considerable effort was made to ensure that our design fits that particular design of ITER. Some features are therefore different from earlier proposals and also incompatible with, for example, the divertor configurations used in simulations by B2-Eirene or EDGE2D/NIMBUS, which use an older divertor design. Inevitable changes in the

present and future ITER designs will require further iterations to determine new suitable sets of lines of sight [2].

The proposed lines of sight are compatible with the reference design of the bolometer detectors [1,3,4]. They are also compatible with other possible compact bolometers, such as the proposal by Di Maio [1,5,6]. These technical matters and questions about materials (radiation hardness), wiring and electronics are not discussed in this report (see Refs. 1, 3 and 4 for a discussion).

The structure of this report is as follows. A brief introduction to tomography methods and a number of matters relevant to tomography on ITER is given in Sec. 2. Section 3 discusses the emission profiles that can be expected in ITER and Sec. 4 the design for the lines of sight for the ITER bolometers. Phantom simulations to assess the performance of this system, and for comparison systems with different numbers of lines of sight, are presented in Sec. 5 and the results are discussed in Sec. 6.

## 2. TOMOGRAPHY METHODS

### 2.1 Tomography problem

Tomography is the reconstruction of local quantities, such as the emissivity, from measurements along lines. In this report we consider two-dimensional emission tomography in a poloidal cross-section of the tokamak. We assume that the measurements are along straight lines, i.e. refraction is negligible, and that the plasma is optically thin. The latter assumption is justified because the main contributions to the total radiated power are from bremsstrahlung and line radiation in the ultra violet. If the plasma is not entirely optically thin for some spectral line in the divertor, the consequences for the reconstructed total radiation will be minor.

The line-integrated measurement $f$ of the emissivity $g$ is given by the Radon transform

$$f(p,\xi) = \iint g(x,y)\,\delta(p + x\sin\xi - y\cos\xi)\,\mathrm{d}x\,\mathrm{d}y\,, \tag{1}$$

where the integral is over the entire region where $g(x,y)$ is non-zero (a region with radius $a$), and $\delta$ is the Dirac delta function. The line of sight is parametrized by $p$ and $\xi$, $p$ being the (signed) distance of the line to the origin and $\xi$ the angle of the line with the positive $x$ axis. The tomography problem is the inversion of Eq. (1), which is an ill-posed problem [7]. In a poloidal cross-section of ITER $x$ corresponds to the major radius $R$ and $y$ to the height $Z$.

Methods to invert the Radon transform are discussed in Sec. 2.3. One way is to discretize Eq. (1) to give a system of equations

$$f_i = \sum\nolimits_j K_{ij} g_j\,, \tag{2}$$

where $f_i$ is the measurement of detector $i$, $g_j$ are coefficients of an expansion of the emissivity on basis functions, and $K_{ij}$ are geometric matrix elements that describe the measuring system. A common choice of basis functions is pixels, in which case $g_j$ is the average emissivity in pixel $j$.

Usually, the system of equations (2) is underdetermined because there are more unknowns (pixel values $g_j$) than knowns (measurements $f_i$).

The above formalism can be extended to three dimensions. In that case, however, a very large number of measurements from all directions is required, which seems impossible in ITER. When toroidal symmetry can be assumed, it is possible to include the lines of sight projected onto the poloidal cross-section into Eq. (2). Toroidal lines of sight are briefly discussed in Sec. 6.1.

### 2.2 Projection space

The parameters $p$ and $\xi$ of the line in Eq. (1) are the coordinates of a new space, which is often referred to as projection space. In this space each line in $(x,y)$ space is represented by a point. The graphical representation of $f(p,\xi)$ in this space is referred to as sinogram; whereas the graphical representation of $g(x,y)$ in $(x,y)$ space is called tomogram. The name sinogram originates from the fact that a delta function in $(x,y)$ space appears as a sine curve in projection space, as is easy to see from Eq. (1). Usually it is sufficient to choose the ranges $p = [-a,a]$ and $\xi = [0,\pi]$ because of the property $f(p,\xi+\pi) = f(-p,\xi)$, which means that the result of Eq. (1) does not depend on the direction of the integral along the same line. However, because the innermost wall of ITER does not have a convex shape this is no longer true everywhere: the path of some lines of sight is blocked by internal structures (notably the separation between the divertor legs). It is important to consider this for the coverage of projection space. It is convenient to extend the range to $\xi = [0,2\pi]$ and to consider the directional $(p,\xi)$ parameters, i.e. to take into account the direction along the line. Specifically, we define the direction $(p,\xi)$ as the direction along the line starting from the circle with radius $a$. For most detectors this definition gives the actual viewing direction along the line, but for a line of sight starting in the separation between the divertor legs the direction is the reverse. The projection space of a poloidal cross-section of ITER can be divided into four regions (see Fig. 1): (1) the region where the direction of the line of sight does not matter with $\xi = [0,\pi]$ (white in Fig. 1), (2) the region where the direction does not matter with $\xi = [\pi,2\pi]$ and hence is the "mirror image" of region 1 (i.e. it carries no additional information) (light grey), (3) the regions where the direction does matter because lines of sight are in the shadow of inner wall structures (grey), and (4) the

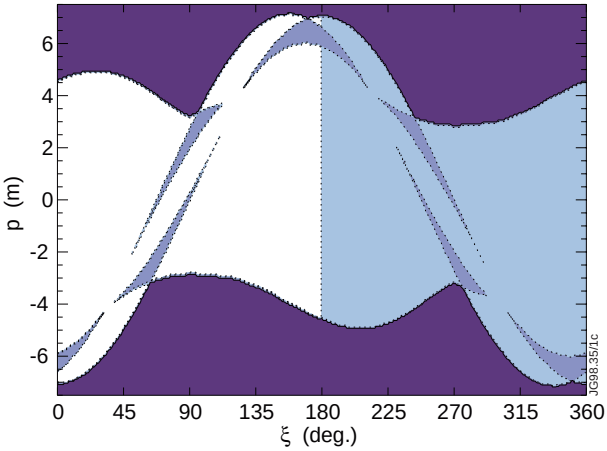


*Figure 1 Separation of projection space into various parts. White: region in which the direction of lines of sight does not matter with ξ = [0°,180°]. Light grey: mirror region in which the direction of lines of sight does not matter with ξ = [180°,360°], which carries no additional information to the white region. Grey: shadow regions in which the direction of lines of sight does matter because internal wall structures block their path. Dark grey: region in which lines of sight do not pass inside the inner wall. For this figure the origin was chosen on the magnetic axis.*

region where no lines go through the region inside the wall and measurements would essentially be zero (dark grey). For a good coverage it is essential that region 1 and all regions 3 are covered well by lines of sight (region 1 automatically gives coverage of region 2). These complications in projection space due to the concave inner-wall shape have several implications for the application of tomography methods. Note that the coordinates of projection space depend on the origin chosen. The effects of choosing a different origin are discussed later.

### 2.3 Tomography methods

Tomography is the inversion of Eq. (1). Although an analytical inverse exists, this is difficult to implement directly for discrete data. However, modifications to the analytical inversion formula exist that can be implemented relatively easily, such as for example in the Filtered Back Projection (FBP) method [7] that is much applied in medical tomography. The main property of these so-called transform methods [8] is that the inverse is expressed analytically, after which the problem is discretized. The main other way to solve the problem for discrete data is by Eq. (2), in which the discretization is done before the inversion. The latter methods are called series-expansion methods [9].

In general, algorithms for transform methods have to be developed for specific applications, and are usually most suited for systems with many lines of sight (>1000) with a regular coverage. Furthermore, many of these methods make specific use of properties of projection space, and would therefore have to be adapted for the complications arising from the concave inner-wall shape in ITER. Also the Cormack method [10], which has been much applied to soft x-ray tomography in fusion research in the past, cannot be applied directly due to the concave inner wall shape. Series-expansion methods are more flexible, they can for example cope with irregular coverage and various *a priori* information required to complement the small number of lines of sight usually available in fusion research, and are used routinely for bolometer and soft x-ray tomography on many fusion devices. Because a well-developed series-expansion method existed which was suited to the problem, this particular one was used in the phantom simulations described in this report (see next subsection). Phantoms are assumed emission profiles that are used in simulations to assess the capabilities of the combination of a measuring system and a tomography algorithm. The complications in projection space due to the non-convex inner wall shape do not rule out the application of flexible transform methods in the future, such as, for instance, the method described in Ref. 11.

### 2.4 Constrained optimization method

The applied series-expansion method uses Eq. (2) and basis functions that describe a bilinear interpolation between grid points. It is a regularized method that is given as a constrained optimization problem, where a functional that describes the unsmoothness of $g$ is minimized with the measurements and estimated noise as constraints. The regularizing functional describes anisotropic smoothness on flux surfaces. Details of the method are given in Ref. 12. The

algorithm is based on a method originally developed by Fuchs [13]. The algorithm described in Ref. 12 has been extended for bolometer tomography at JET, notably by a way to take into account the effect of charge-exchange neutrals on the signals of some bolometers [14]. Furthermore, for bolometer reconstructions, both for JET and the simulations for ITER, it is very important to make use of the non-negativity constraint that is available in the algorithm, because otherwise reconstructions with significant negative artefacts are obtained. Similar methods are used for soft x-ray tomography at JET [12] and other tokamaks [15], and also in other fields [16].

One feature of the implementation that is important for the ITER simulations is the possibility to have a varying grid size in different parts of the cross-section. In the divertor smaller structures are expected than in the bulk plasma. Therefore, the distance between lines of sight that see the divertor is chosen to be much smaller than those that see only the bulk plasma. To resolve the features, and to make solutions possible that are consistent with all line-of-sight measurements, a small grid size is required. The complexity of the problem increases with the number of unknowns, i.e. the emissivity in the $N$ grid points, compared to the knowns. Furthermore, the time to find a solution is roughly proportional to $N^3$. Therefore, to minimize the total number of grid points, the grid is chosen according to the average distance between lines of sight, i.e. smaller in the divertor than in the bulk plasma. A high resolution is also required in the edge and scrape-off layer of the main plasma. Although lines of sight have been chosen accordingly, in the present simulations the grid size has not been reduced in the edge. Although it is technically possible to do this in the current implementation, this was not done because the expected gain in information from these preliminary simulations did not justify the effort to design such a grid.

The memory and CPU time consumption of the tomographic reconstructions depend mainly on the number of grid points. The finest grid used, with about 3300 grid points, stretched the computing facilities available for the simulations (an IBM RS6000 workstation with 128 Mbyte of memory) to the limits. Despite an implementation of sparse-matrix storage, the memory requirements go roughly with $N^2$ and the memory limits were reached. The CPU time for one reconstruction was typically 12 hours. To be able to make more simulations, the fine grid has only been used for some simulations and a finer grid of about 1500 points was used in most simulations (typically 1–2 hours of CPU time). These limitations would not appear on more powerful computers. At the time when reconstructions of actual ITER plasmas will be required, the expected increased performance of computers will have alleviated the main present problems.

## 3. PHANTOMS

We will describe the requirements of the system in terms of the expected emission profiles (phantoms) that one should be able to reconstruct reliably. A large part of the radiation is emitted from the divertor. The quantification and localization of this radiation is an important aim of the bolometer diagnostic.

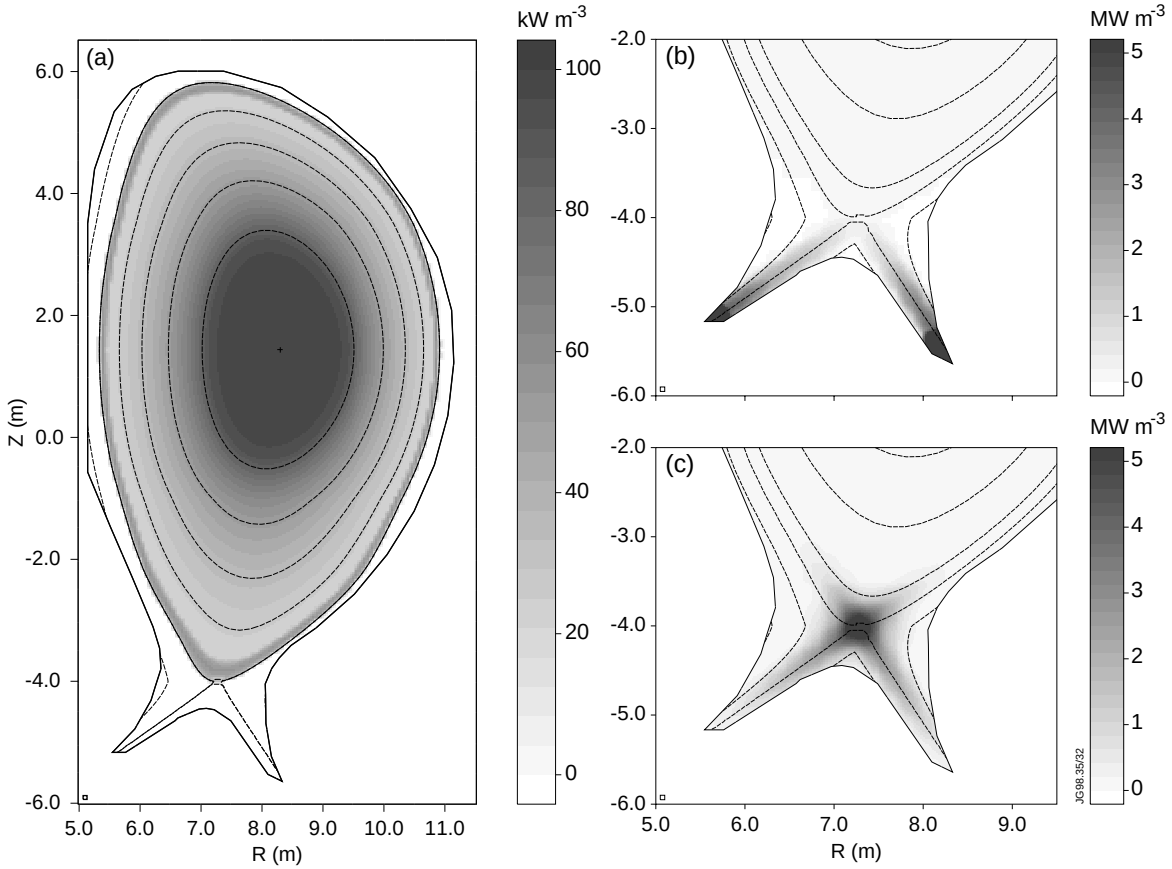


*Figure 2 Phantoms of (a) bulk radiation, (b) radiation in a partially attached plasma and (c) radiation in a fully detached plasma. The dashed lines indicate flux surfaces. Note that the phantoms in (b) and (c) contain the bulk radiation of (a), but that this is hardly visible because the radiation level in the divertor is more than one order of magnitude higher than the bulk radiation. In particular, the phantom in (b) has even higher peaks at the strike points, which are not visible in the grey-scale plots because the range was chosen such as to clearly show other structures. The small boxes in the lower left corners indicate the grid size used in the divertor region.*

To cover the range of (divertor) emission profiles that can be expected in ITER we have chosen two widely different phantoms: a partially attached case [17] and a fully detached case [18], see Figs. 2(b) and (c), respectively. Both are based on B2-Eirene simulations. Unfortunately, the divertor shape used in these simulations does not correspond to the latest geometry that has been used for our design. Therefore, for the phantoms the main features of the B2-Eirene simulations were described as a combination of analytical functions. The bulk radiation in ITER is expected to have a broad peak in the centre and a sharp localized peak at the edge [19]. A bulk phantom was constructed with these characteristics that has constant emission on flux surfaces, see Figs. 2(a). This bulk phantom is incorporated into the other phantoms. The magnetic configuration in ITER is expected mainly to vary in the upper inner corner [20], see Fig. 3. The sinograms of the bulk radiation and the total radiation of the two phantoms are shown in Fig. 4. It is evident that especially the sine-like bands, high values originating from the divertor region, have to be covered well, including the shadow regions. Furthermore, the bulk plasma should be covered at least coarsely, and the edges finely. The shape of the sinograms depends on the choice of the origin. For Fig. 4 the magnetic axis was chosen for the origin. If, on the other hand, the X

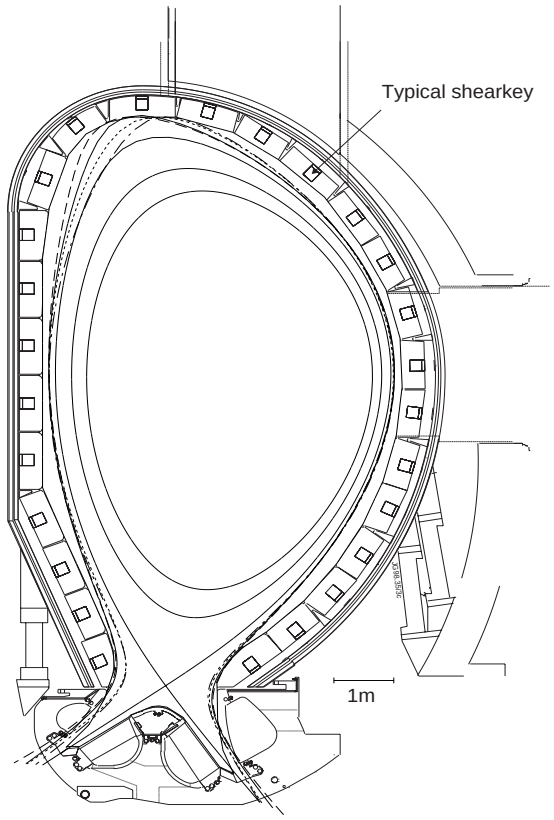


*Figure 3 The current ITER first-wall design and the location of ports. The shear keys are shown in the blanket modules. Typical magnetic flux surfaces are shown as solid lines. In the upper-inner corner the extent of the plasma for a number of configurations are indicated by dashed and dashed-dotted lines.*

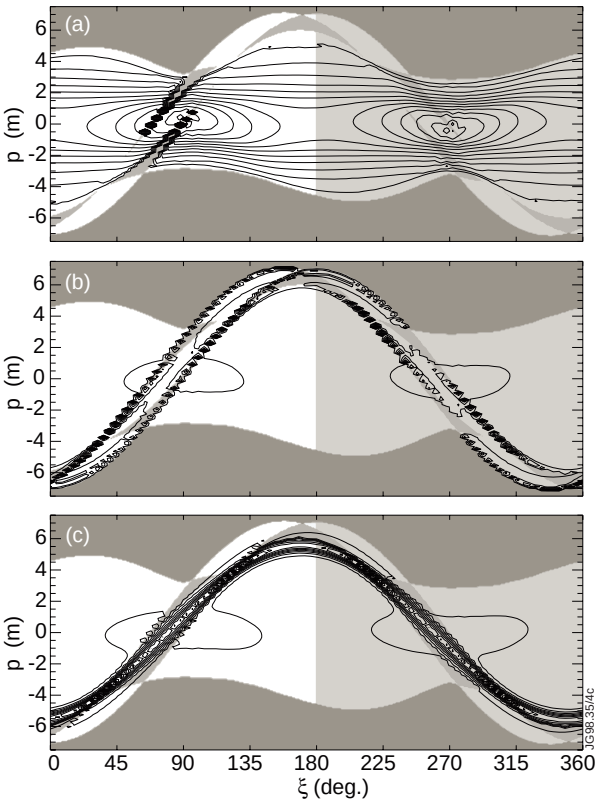


*Figure 4 Sinograms of the phantoms in Fig. 2(a-c). The contours were chosen according to the maximum value for each phantom and are therefore not the same in (a-c). The origin of the projection-space coordinates was taken on the magnetic axis. Note the discontinuities that the shadow regions cause in the sinograms.*

point is chosen as the origin, the sinogram has a simpler shape (see Fig. 5). Although the choice of the origin in the X point is more natural because the peak emission is there and the sinogram has a simpler shape, the scale in *p* is stretched to include the entire plasma. Because it gives a more balanced view, we have chosen to present the projection-space images with the origin on the magnetic axis, unless it is clearer to do otherwise.

There are a number of complicating effects. In JET a significant contribution of charge-exchange neutrals to the measurements of bolometers in the divertor has been found [14,21]. A tomography method was

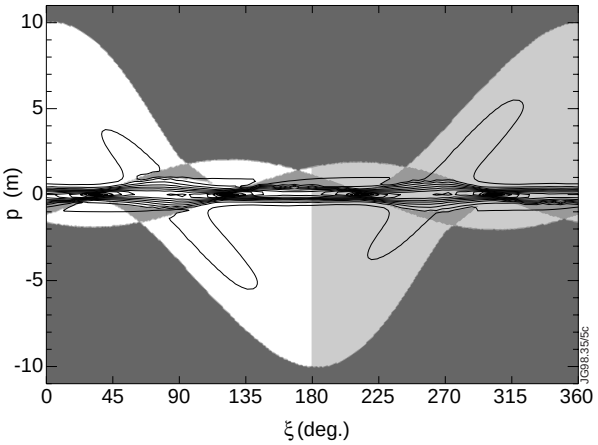


*Figure 5 Sinogram of the phantom in Fig. 2(c) with the origin of projection-space coordinates in the X point [cf. Fig. 4(c)].*

developed to distinguish the neutral part from the electromagnetic radiation part based on the comparison of measurements of divertor radiation from both outside and inside the divertor [14]. The contribution from neutral particles is seen to increase with closure of the divertor (going from the open MkI divertor to the more closed MkIIA divertor). The measurements are supported by EDGE2D/NIMBUS simulations. A significant part of the radiated power loss is carried by neutrals. The method to estimate the neutral contribution to the bolometer signals gives information of this power loss. Since ITER has an even more closed divertor, very large contributions from neutrals on the divertor bolometers can be expected in ITER. The divertor bolometers are a very useful tool to measure the neutrals in the divertor, which may play an important role in the power balance and to wall loading. Therefore, care should be taken in the design of the bolometer system that the separation between electromagnetic radiation and neutrals is also possible inITER.

Another complicating effect is that measurements in reality are not along lines as assumed in Eq. (1), but along strips with a finite width. In particular the cameras that view the plasma through toroidal gaps between blanket modules (see Sec. 4.1) are required to have appreciable extent in the poloidal direction (about 10 cm at the blanket surface, extending to up to a metre on the other side of the plasma) to have a good signal-to-noise ratio, assuming noise levels of the JET bolometers, see Ref. 3. In the present tomography methods it is possible to take into account these beam widths [12]. For the sake of simplicity the beam widths have not been taken into account in the simulations presented in this document because to do so a detailed design of the detectors would be required and because the detectors may still be improved to be more sensitive. The beam widths will have some adverse effects on the attainable resolutions, but this is not expected to be of major importance. If a number of detectors have overlapping beam widths, ways exist to restore the underlying smoothed information, see for example Ref. 22 and references therein.

## 4. CRITERIA

The criteria for choosing lines of sight have been: (1) the capability to make tomographic reconstructions without stringent assumptions of the emission, and (2) taking into account the technical constraints. The first criterion requires a large number of lines of sight and a good coverage of important regions. The second criterion includes the availability of space, connectors and cables, access for maintenance, radiation protection, etc. The location of the proposed lines of sight are shown in Fig. 6(a) and the corresponding coverage of projection space in Fig. 6(b). The considerations that led to this design are discussed next.

The important regions to cover are the X point and divertor, the edge of the bulk plasma, and the bulk itself (which is important for the total emitted power calculation.). It should be understood that it is usually not possible to reconstruct parts of the emission separately because lines of sight view through other regions, so that adequate coverage of all parts is essential. An exception can be the bulk radiation as will be discussed later. A main factor determining how

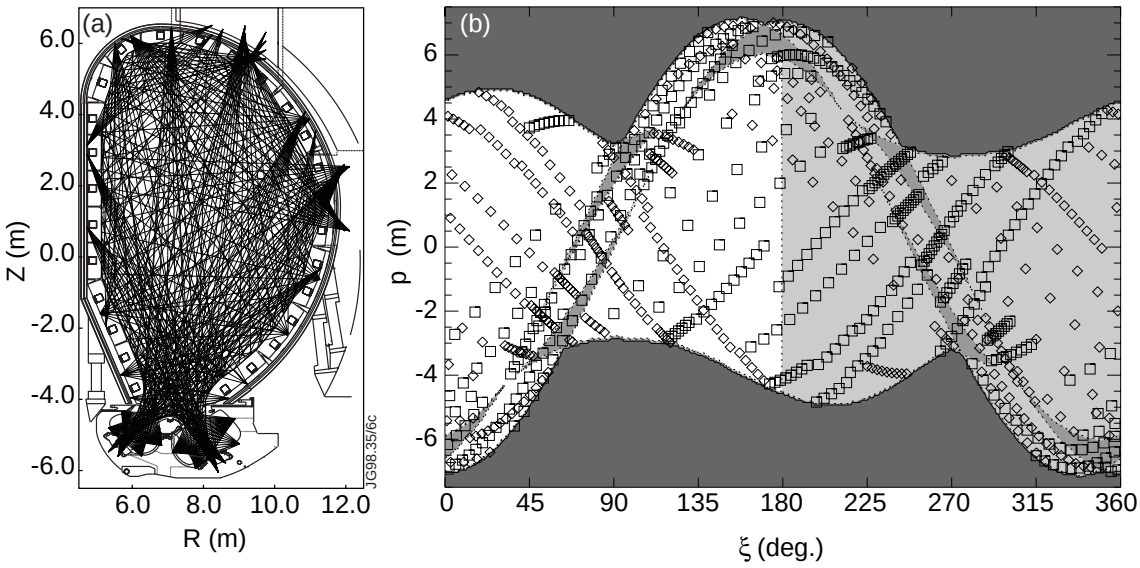


*Figure 6 (a) Proposed lines of sight for bolometry on ITER. The ITER structure is shown (note the shear keys in the blanket modules). (b) Coverage of projection space by the proposed lines of sight. Squares indicate the directional view of each line of sight, the diamonds the mirrors of the lines of sight for which the direction is not relevant. To determine the quality of the coverage it is sufficient to consider squares and diamonds in the white region and points (squares) in shadow regions.*

good a choice of lines of sight is for tomography, is the coverage of projection space. The cameras (projections) should be spread out evenly over all angles. An asymmetric coverage and gaps will lead to artefacts, unless much *a priori* information can be implemented in the tomography algorithm. Due to the complex structure of the divertor it is essential to have good views into the divertor legs. The number of projections determines roughly the angular resolution of structures [10,23]. We have chosen this number on basis a reasonable coverage of projection space and what seems technically feasible. Note that this results in fewer projections than would be required for tomography if no *a priori* information at all can be assumed. The number of channels determines the size of structures that can be resolved [10,23]. The resolution can be close to the spacing between channels only if a large number of projections, i.e. angles, are available (see Sec. 5.2 for a discussion on resolution). The actual obtainable resolution by the system has to be assessed by means of phantom simulations. In this way the requirements of resolution can be translated into the required total number of bolometers. Given the limited resolving power of the present bolometer tomography systems on JET and ASDEX-Upgrade, which have of the order of 100 channels, one should aim for at least double that resolution. Because it is a two-dimensional problem, it is evident that double the resolution requires double the number of viewing directions and double the number of lines of sight per viewing direction. We think, therefore, that the absolute minimum number of lines of sight required to resolve features with sizes as small as 10–20 cm is 400, which also seems to be technically feasible. Resolving smaller structures would require low-noise measurements from several thousands of lines of sight from tens of angles (cf. medical x-ray tomography). As many as possible views should fit in one poloidal cross-section to avoid problems with possible toroidally asymmetric emission.

The lines of sight can be divided into groups. For technical purposes the bolometers can be grouped according to their location: the blanket, the divertor and the ports. For tomography it is more useful to group the bolometers according to their function: coverage of X point and divertor, coverage of the bulk, and coverage of the bulk edge. Both of these groupings are used in the following.

### 4.1 Technical considerations

One important problem with the reference design of the bolometers is that each channel requires four cables to function (two cables supplying the input voltage, and two for the measurement). Several hundreds of channels lead to of the order of one thousand cables and equally many feedthroughs.

The horizontal and vertical ports are the most favourable locations for bolometers. Although the bolometers have to make parasitic use of ports allocated to other diagnostics, their small size poses no problems. Wiring of the cables and the location of feedthroughs seems to be most favourable in the ports. Furthermore, if bolometers are damaged, the ones located in a port stand most chance for repair. Therefore, a large number of channels with an as large as possible coverage have been chosen. The bolometers in the horizontal port are located on the sloping faces of the neutron camera pre-collimator, whereas the bolometers in the vertical port are located in diagnostic tubes that reach in as far as possible.

The ports only do not allow a sufficient coverage because the angles are rather limited. More angles of coverage are required for a proper reconstruction of the X point and divertor. Therefore, bolometers at the rear of the blanket modules are envisaged, making use of diagnostic sockets for electrical connections and the thickness of the blanket for radiation protection (also profiting from the cooling of the blanket modules). These bolometers view the plasma through the 2-cm wide gap between blanket modules. The views are limited severely by shear keys between blanket modules [see Fig. 6(a)]. The number of blanket cameras and their location has been determined by the number of connectors and their pins that are planned (see Sec. 6.1 for sector allocation).

Only a very limited view of the divertor is possible from outside the divertor. Therefore, it is very important to have bolometers located inside the divertor, viewing the plasma through tile gaps. A relatively large freedom has been assumed in the location of divertor bolometers.

Because the detectors are so small, four channels in a box of $3316 \times 30$ mm$^3$ plus space for collimators, no special consideration was required for the spacing between detectors.

Reference 4 gives more technical details on the bolometers and their implementation in ITER.

### 4.2 Choosing the coverage

The largest part of the radiation is expected to originate from the X point and the divertor legs, and radiating structures in these regions will be of most interest. In projection space the

radiating divertor region will give rise to a roughly sine shaped structure, see Fig. 4. Therefore, a regularly spaced set of views of the X point and divertor has been made, Fig. 7. The views from the inner and outer wall, that look deep into the divertor legs are particularly important. Gaps in the coverage are due to technical limitations. There will also be radiation from the edge of the bulk plasma, especially in a thin layer. To be able to resolve this thin layer, a number of views of the edge with fine coverage has been implemented (see Fig. 8). In the upper-inner corner these views should be able to detect the change in magnetic configuration (Fig. 3).

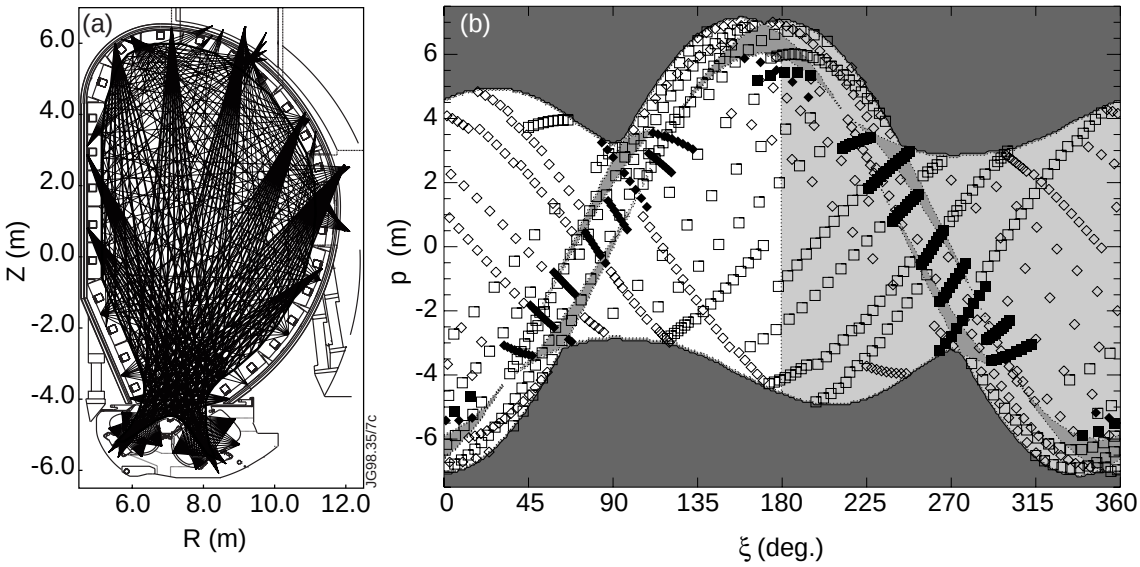


*Figure 7 (a) Positions and (b) projection-space coverage of lines of sight that view the X point and divertor from around the main plasma. These lines of sight are highlighted, while the other ones are shown for reference.*

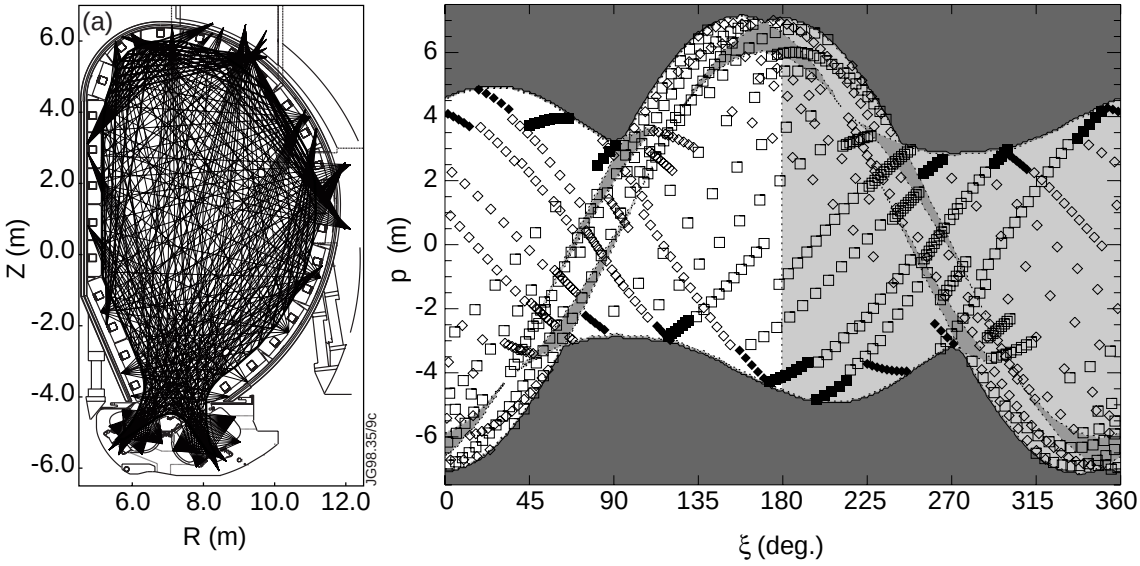


*Figure 8 (a) Positions and (b) projection-space coverage of lines of sight that view the edge of the bulk plasma.*

Divertor cameras are required to fill shadow regions in projection space and for good local coverage of small structures, see Fig. 9. However, there should also be a sufficient coverage of the divertor legs *without* the divertor cameras to allow for rough reconstructions in cases when

divertor bolometers cannot adequately measure the radiation (for example when a large number of neutral particles are produced or the pressure near the bolometers is very high), or when divertor bolometers break. To signal these problems it is very useful to have some lines of sight from the divertor bolometers that coincide with other lines of sight. A minimal set of two roughly perpendicular views per leg is indicated by P in Fig. 9(a).

To fill gaps in projection space (mainly the bulk region), full coarse fans were chosen instead of single channels because neighbouring channels can be used to assess the reliability of channels and because the loss of single bolometers will have less damaging consequences since information from the neighbouring channels will still be available. These bulk channels are shown in Fig. 10. The most important views are from the ports and from two views (inside and outside) from the blanket in the lower part of the cross-section.

The coverage of the blanket cameras and the cameras in the two ports are shown separately in Fig. 11. There should be at least one approximately full projection so that a reliable measure of the total emitted power can be obtained without tomographic inversion. Furthermore, some divertor lines of sight should overlap with lines of sight from outside the divertor to enable a comparison that gives information on neutral effects. Table I summarizes the proposed lines of sight. The numbers give an indication of the requirements, but the number of channels per view could be varied to a limited extent in the final design without significant consequences to the conclusions in this report. Priorities of the lines of sight are discussed in Sec. 6.2.

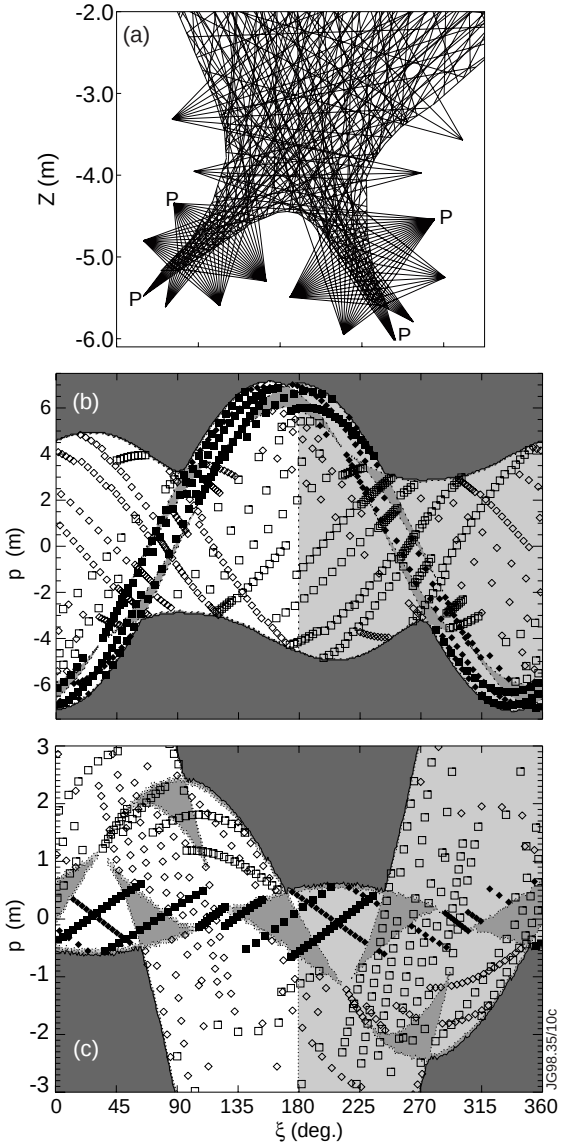


*Figure 9 (a) Positions (an important subset of views is indicated by P), (b) projection-space coverage, with the origin on the magnetic axis, of lines of sight that view from around the divertor. (c) For clarity the projection-space coverage with the origin in the outer divertor leg of lines of sight that view from around the outer divertor leg.*

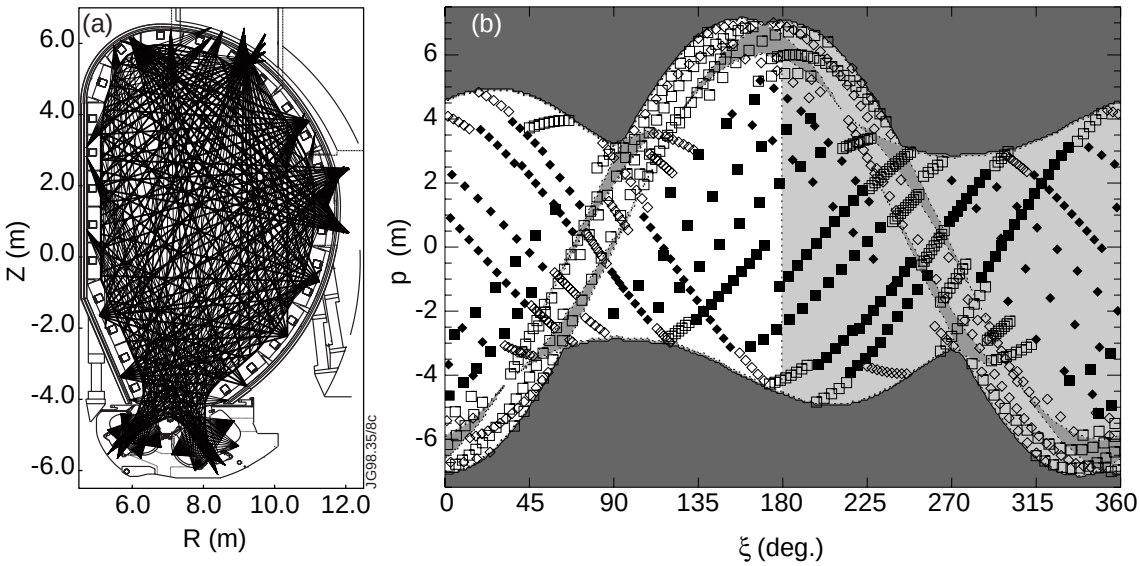


*Figure 10 (a) Positions and (b) projection-space coverage of lines of sight that view the bulk plasma.*

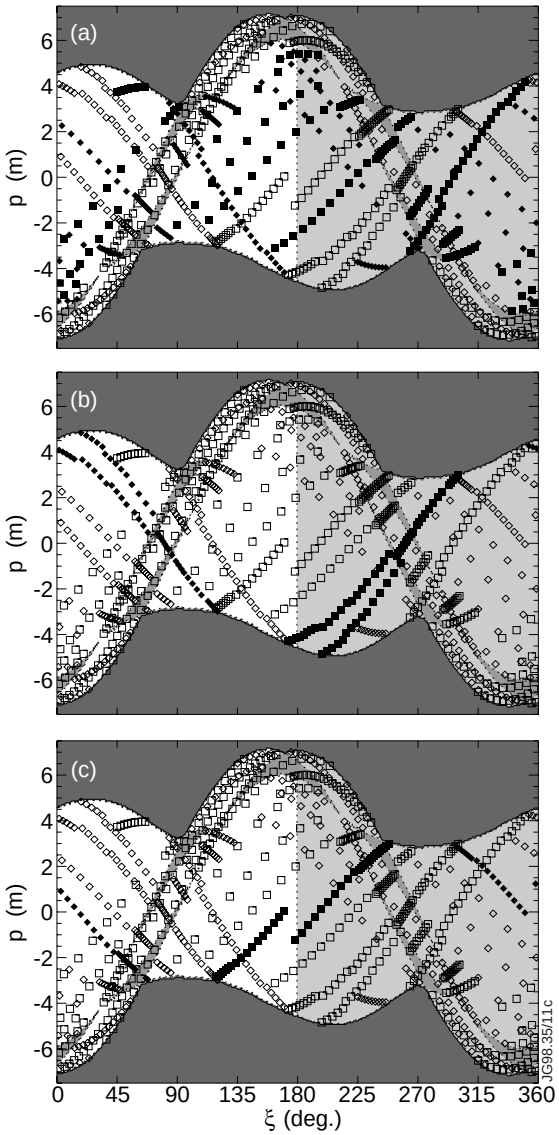


*Figure 11 Projection-space coverage (origin at magnetic axis) of lines of sight of (a) cameras in the blanket, (b) cameras in the vertical port, and (c) cameras in the horizontal port.*

***Table I*** *Proposed numbers of lines of sight for tomography in one poloidal cross-section.*

| Location | Description | | Number of lines of sight |
|---|---|---|---|
| Horizontal port | 1 X-point and lower edge fan | | 15 |
| | 2 bulk fans | | 10+10 |
| | 1 fine upper-edge fan | | 7 |
| | | subtotal | 42 |
| Vertical Port | 1 X-point fan | | 10 |
| | 6 parts of bulk fans | | 5+5+4+4+4+4+5 |
| | 3 fine-edge fans | | 5+5+8 |
| | | subtotal | 59 |
| Blanket | 8 X-point and edge fans | | 5+9+9+9+9+11+9+5 |
| | 7 bulk fans | | 9+9+14+11+9+9+4 |
| | 4 edge fans | | 4+9+5+5 |
| | | subtotal | 154 |
| Divertor | 6 fans outer leg | | 20+10+10+10+15+20 |
| | 6 fans inner leg | | 20+15+10+10+15+15 |
| | | subtotal | 170 |
| | | total | 425 |

## 5. PHANTOM SIMULATIONS AND ASSESSMENT OF THE IMPORTANCE OF LINES OF SIGHT

Phantom simulations have been carried out to assess the minimum resolution that should be obtainable with the proposed bolometer system for ITER using a state-of-the-art tomography method (see Sec. 2.4). Furthermore, the effects of using fewer lines of sight have been investigated. It is difficult to use these simulations to prioritize the lines of sight, because if it is decided that certain cameras or the total number of lines of sight are not feasible, the remaining lines of sight should be optimized to compensate as much as possible for the lost information. In these simulations, therefore, we focus on the general effect of fewer or more lines of sight and effects due to the accidental loss of a whole range of cameras. The separate issue of priority of lines of sight has therefore been addressed based on theoretical considerations (coverage of projection space) and on our experience at JET, see Sec. 6.2.

Although improvements in the reconstructions can be expected by optimizing the tomography method for the lines of sight and expected emission profiles, the simulations show what should be possible and give a clear indication of the effect of using fewer lines of sight.

### 5.1 Description of simulations

The tomographic reconstruction method and the grids used were discussed in Sec. 2.4. In the simulations pseudo-measurements are calculated given the lines of sight and the phantoms. Gaussian noise is added to the pseudo-measurements to simulate experimental conditions. Both

relative noise and absolute levels have been tried, with only minor differences in results. In the results presented here relative noise with a standard deviation of 1% was assumed.

In phantom simulations a reconstruction error can be defined as

$$\sigma_g = \frac{\|\boldsymbol{g} - \boldsymbol{g}_0\|}{\|\boldsymbol{g}_0\|},$$

where $\boldsymbol{g}_0$ denotes the phantom values in the grid points and $\|\cdot\|$ the Euclidean norm. This reconstruction error quantifies the relative deviation of the reconstruction from the phantom. With difficult phantoms with large peaks and a tomography system with only a few hundred lines of sight reconstruction errors of up to 50% or even larger are not uncommon. In such reconstructions the important features may still be reconstructed well. Another good quantifier to compare is the total radiated power of the phantom and of the reconstructions.

### 5.2 Resolution

There can be confusion over what is meant by the resolution of a system. A proper definition of resolution is the smallest structure or the smallest separation between two small structures that can still be resolved by tomographic reconstruction, taking into account a realistic noise level and other sources of uncertainties. Following the experience of medical x-ray tomography where thousands or even tens of thousands of lines of sight are available (by rotating arrays of detectors around the patient) to achieve millimetre resolution, a similar number of lines of sight with regular coverage could give a resolution of 10–20 cm in ITER, assuming very little noise. Obviously, the resolution defined in this way would be different in different parts of the plasma. Note that this definition of resolution, i.e. by what is actually resolvable by tomography, gives extremely different requirements than the “resolution” that is sometimes taken as the typical distance between lines of sight from a very limited number of directions. We are still able to achieve reasonable reconstructions with a very limited number of lines of sight by taking into account *a priori* information that biases the solution in a direction that is physically meaningful.

Because with the very limited number of lines of sight and number of views that seem feasible for bolometry in ITER, the above definition would give numbers that are not very meaningful, we have chosen the following description of the required resolution: the main features and, to a certain extent, details of realistic emission phantoms should be resolvable. This means that one compares the main features of phantom simulations by eye, and compares the magnitudes of features by the overall reconstruction error.

### 5.3 Overview of simulations and discussion

Simulations were carried out with the phantoms described in Sec. 3. The results are summarized in Table II. The reconstructions with all the proposed lines of sight serve as a reference. The different cases studied are described below.

***Table II*** *Reconstruction errors and reconstructed total emitted power of phantom simulations with a varying number of lines of sight for two phantoms*

| Simulation type | partially attached phantom | | fully detached phantom | |
|---|---|---|---|---|
| | $\sigma_g$ (%) | $P_{tot}$ (MW) | $\sigma_g$ (%) | $P_{tot}$ (MW) |
| Phantom | – | 227 | – | 250 |
| All channels | 56.2 | 225 | 20.5 | 250 |
| Every sceond channel | 58.9 | 224 | 24.2 | 249 |
| Priority channels | 78.5 | 235 | 42.4 | 248 |
| No blanket channels | 66.6 | 216 | 21.9 | 245 |
| No divertor channels | 85.8 | 226 | 33.0 | 248 |
| With neutrals | 85.5 | 233 | 44.2 | 261 |
| 1400 channels | 53.5 | 231 | 7.5 | 250 |

*5.3.1 All lines of sight*

Figures 12(b) and 13(b) show the divertor region of reconstructed emission profiles. The phantoms of Fig. 2 are shown again in Figs. 12(a) and 13(a). The agreement in structures is good and seems to be adequate. However, the peak values are not reconstructed accurately. In particular in the partially attached case, where very high localized radiation peaks exist at the strike points, the discrepancy accounts for most of the relatively high reconstruction error. The total radiation is reconstructed very well (within 1%).

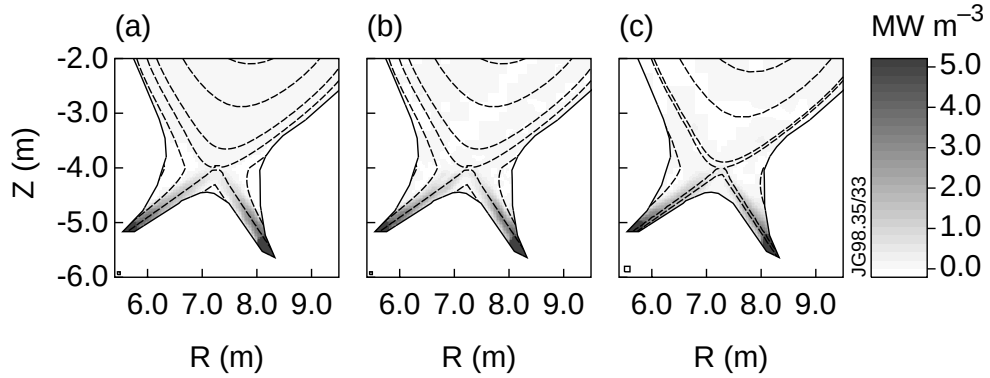


*Figure 12 Reconstructions of the partially attached phantom around the X point. (a) Phantom, (b) reconstruction with all lines of sight, and (c) reconstruction without blanket cameras.*

The emission in the bulk plasma is not reconstructed well: large oscillations exist. This is due to the large difference in emission values in the bulk and in the divertor: because many lines of sight view the divertor through the bulk radiation, small errors in the divertor radiation lead to relatively large variations in the reconstructed bulk radiation. This is also the main problem for bolometer reconstructions in JET, where only about 85 channels are available. The problem is

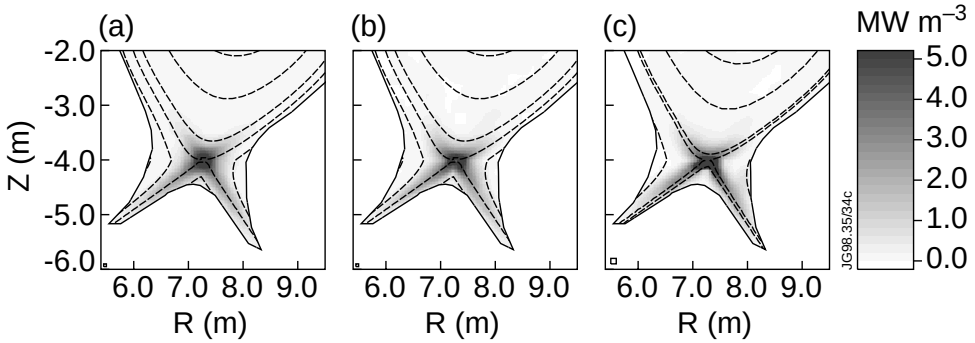


*Figure 13 Reconstructions of the fully detached phantom around the X point. (a) Phantom, (b) reconstruction with all lines of sight, and (c) reconstruction with neutral particles.*

not exclusively due to the added noise to the pseudomeasurements: relative and absolute noise both show the same problem. Apparently, these problems have very little effect on the reconstructed total radiation, half of which is radiated from the bulk. This is also the experience from JET.

*5.3.2 Independent reconstruction of bulk radiation*

In the present tomography method with the current parameters the bulk radiation cannot be reconstructed well if the lines of sight that see the divertor are included in the reconstruction. There is, however, a sufficient number of lines of sight that view the bulk without seeing the divertor. In the partially attached case a very good reconstruction of the bulk radiation is obtained when only these lines of sight are used ($\sigma_g = 13.9\%$, and the total radiation of 108 MW of the bulk phantom matched). It is likely that the result would be even better if a fine grid on the edge were used in order that the steep gradients at the edge can be represented on the grid.

If the main radiation peak is close to the bulk plasma, as is the case in the fully detached plasma, the separation between bulk and divertor radiation is more problematic. However, it still seems feasible to make reasonable reconstructions of the bulk part not affected by the divertor.

*5.3.3 Half of the lines of sight*

In order to show that as many as possible lines of sight should be used in the design, the simulations have been repeated with half the number of channels. If whole cameras would be left out in the final design, the other cameras should be optimized for the new situation. To avoid such complications, every second channel of the proposed system was selected. The main features are still reasonably reconstructed, but, as expected, the reconstruction errors are larger, although the difference with reconstructions with all lines of sight is not dramatic.

When half the lines of sight are chosen from only the “priority” views (see Sec. 4.2 and Table III in Sec. 6.2) instead of choosing every second channel from all views the results are far worse. That the results are even worse than the simulations without blanket views or divertor views indicates that both the bulk and divertor are reconstructed worse. It must be said, however, that the priority views were chosen as a subset from the balanced proposal. If they were

designed more specifically for their task, the results might be better. Furthermore, with more *a priori* information an improvement may also be found.

*5.3.4 No blanket cameras or no divertor channels*

It is likely that at least some bolometers will be damaged during operation. The probability that one can replace bolometers is lowest for the blanket bolometers. Furthermore, divertor bolometer channels may fail due to the harsh conditions. Simulations were done in order to assess what happens if these channels are lost. When no blanket channels are available, the reconstructions are worse than when all channels are used, although the main features can still be recognised, see Fig. 12(c) for the result in the partially attached case. Loss of the divertor channels is more severe, since these give the most accurate information on the features of the divertor radiation. Note that operation without blanket cameras will give very bad results if there is a significant contribution of neutral particles to the signals measured by the divertor bolometers.

*5.3.5 Neutrals*

At JET a way to deal with contribution of the neutral particles to the signals measured by the divertor bolometers has been developed [14]. It is essential that as many X-point and divertor views from outside the divertor as possible are available, in combination with as many as in-divertor views as possible. The reconstruction is heavily biased towards the information of the ex-divertor views. The information of the divertor views that is consistent with the ex-divertor measurements is used to reconstruct the divertor more accurately, and the remaining part of the

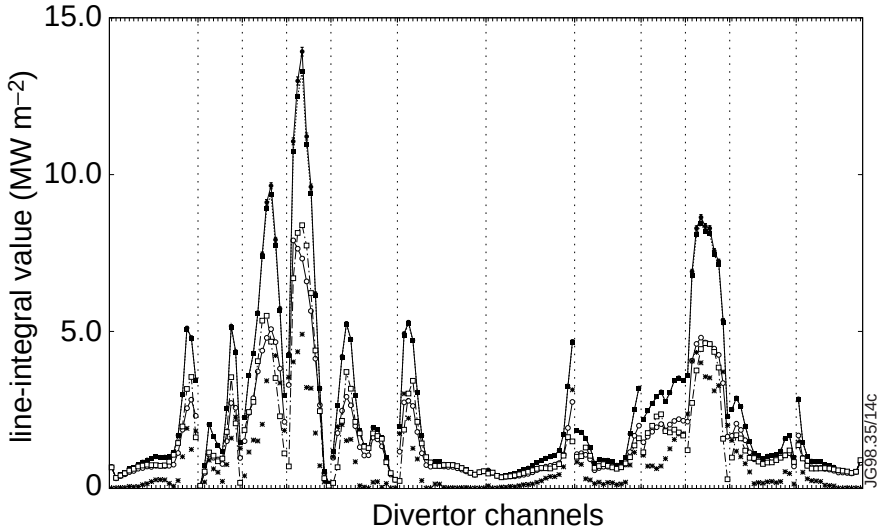


*Figure 14 Pseudo-measurements and back-calculated measurements of divertor channels in a simulation with the partially attached phantom including neutral particles on the divertor channels. Open circles: pseudo-measurement of emitted electro-magnetic radiation. Filled circle: pseudo-measurement including the contribution of neutrals (with estimated errors given as error bars). Filled squares: backcalculated total. Open squares: backcalculated electro-magnetic radiation part. Asterisks: reconstructed neutral contribution. The numbering of channels is clockwise (cameras are separated by a dashed line): first the cameras around the outer divertor leg, and then the ones around the inner divertor leg.*

signal measured by divertor channels is assumed to be from neutral particles. Although it is a crude way of handling the problem, it works reasonably well at JET [14]. In our simulations for ITER the results in terms of the reconstruction error, however, are the same or worse than if the divertor channels are not considered at all. In these simulations a contribution from neutrals was added to the divertor channels which varied between 0 and 100%. The features of the reconstruction are still reasonable [see Fig. 13(c) for the fully detached case], and also the reconstructed level of the neutrals is reasonable (see Fig. 14). It must be stressed that in the simulations the recipe that works for JET was copied to ITER. There is still room for much improvement, for example by more actively comparing the many in-divertor and ex-divertor views that coincide.

*5.3.6 More lines of sight*

It is interesting to compare the results for the proposed system, which has a feasible number of lines of sight, with the results that could be obtained if there was enough freedom for a much larger number of lines of sight. For that purpose we made an "optimum" regular coverage of projection space where the distance between points is related to the expected sizes of structures in various regions of projection space, see Fig. 15 (cf. the proposal in Ref. 3). For the bulk and edge regions a so-called interlaced coverage has been used (this should also be used for the X point region in future simulations). Interlaced coverage can save half of the channels, as a theorem from the mathematics of tomography states that the information contained on a regular grid in projection space is also contained in the interlaced coverage: where odd points are taken in every second row and even points in the other rows [24]. As could be expected, the results are significantly better than with the proposed coverage, especially in the fully detached case. In the coverage of Fig. 15 the fine coverage of the divertor region may not be sufficient for the partially attached phantom (in fact, the distance between lines of sight is not much better than in

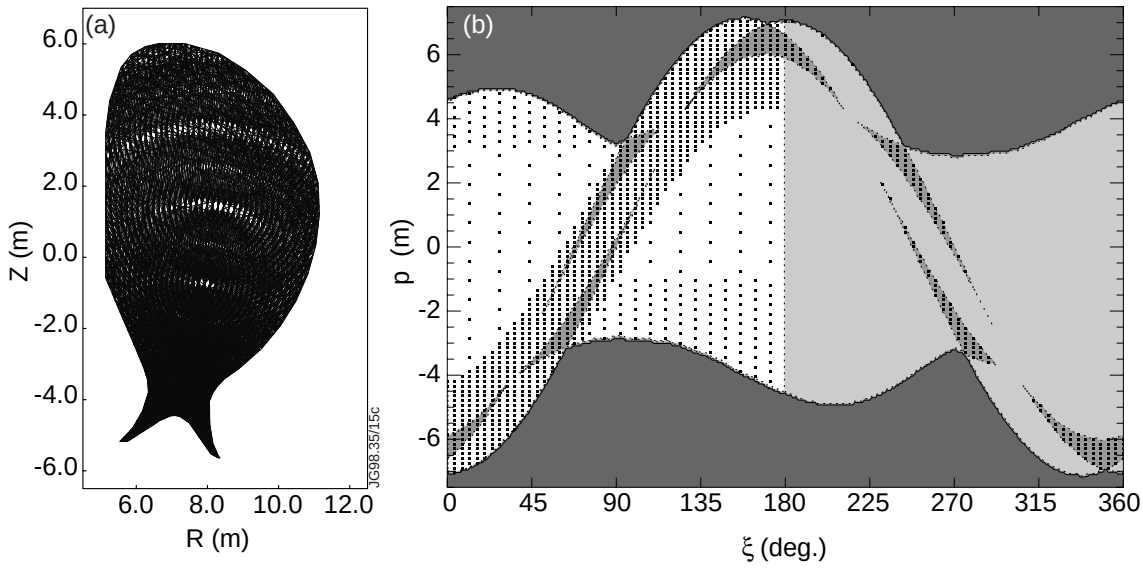


*Figure 15 (a) Positions and (b) projection-space coverage of 1400 lines of sight with optimized "regular" coverage. In (b) only the directional lines of sight are shown.*

the proposed coverage). Furthermore, the grid size used in the divertor may not have been sufficiently small. It is also surprising that even with this number of lines of sight no good reconstruction of the bulk plasma is obtained simultaneously with the divertor radiation.

### 5.4 Conclusions from tomography on line-of-sight coverage

It has been demonstrated that reasonably good reconstructions of the divertor radiation can be obtained when using all lines of sight, but that the bulk radiation is not well reconstructed due to the large difference in magnitude of local emission in the bulk and the divertor. However, there is a sufficiently good coverage of the bulk plasma (when lines of sight that see the divertor are disregarded) that separate good reconstructions of the bulk plasma are possible. Note, however, that a separate reconstruction of only the divertor radiation is not possible because most channels seeing the divertor look through a part of the bulk: due to the larger volume of the bulk the contribution of the bulk plasma to the line-integral values can be of the same order as the contribution from the divertor. Even in the case of 1500 optimal lines of sight the reconstruction of the bulk emission was not good. It should be realised, however, that the simulations were carried out with the tomography algorithm at JET without optimization for the ITER situation. We believe that with the current tomography methods there is sufficient scope for improvement by optimization and possibly the inclusion of more *a priori* information.

The reconstructions with fewer lines of sight show that if channels are lost due to accidental damage still reasonable reconstructions can be obtained. One should not conclude on basis of these simulations that the difference between all lines of sight and half of them is so small that one can settle with the lower number. One should realise that it is likely that the number of lines of sight will be reduced by accidental damage under the hostile conditions in the ITER vacuum vessel. If one starts with the maximum number of feasible channels one has the best chances to extract as much information as possible from the measurements and learn what the characteristics of the ITER plasmas are. At a later stage in the operation of ITER, when more is known about the actual emission in ITER plasmas that can be included as *a priori* information, fewer channels may be sufficient. It remains a problem to separate the neutral contribution and electromagnetic radiation contribution to the signal measured by the divertor bolometers. The simulations show that this is possible to a certain extent with existing methods, but that improved methods have to be developed for better results and a good determination of the power lost due to the charge-exchange neutrals. The simulations also show that for good reconstructions of the radiation near the strike points in attached plasmas a significantly larger number of divertor channels is required than used in the present simulations.

The total power calculation is very good (within 1%), even with limited number of lines of sight or lost views. This is encouraging. There is also scope for a simplified method to calculate the total radiated power from a limited number of lines of sight. For this purpose more vertical lines of sight from the top of the machine would be advantageous.

## 6. DISCUSSION

The locations of the bolometers in ITER, the priorities of the lines of sight, and the general conclusions are discussed. The proposals and conclusions correspond to those in Ref. 1.

### 6.1 Locations in ITER

In the simulations it was assumed that all lines of sight are in one poloidal cross-section. This is probably not possible. The toroidal distance between the various bolometers should be minimized to avoid problems related to possible toroidal asymmetries. Furthermore, sectors where gas inlets are located (sectors 4, 8, 12, 16 and 20) should be avoided altogether since the gas is known to cause toroidal asymmetries in emission. Potential perturbations due to pellets and NBI are considered to be less serious. Diagnostic ports that could be used are the horizontal port in sector 9 and the vertical port in sector 10. Blanket connectors are available in sectors 10 (preferred) and 16, and a limited set in sector 9. The nearest sector with a divertor instrumentation cassette is sector 8, which causes a problem with the gas inlet. It would be highly preferable to modify the cabling of the divertor cassettes in order that the divertor bolometers can also be located in sector 10.

So far, only one main poloidal cross-section has been considered. It would be advantageous to have a subset of important channels in as many as possible other sectors to be able to monitor toroidal asymmetries. Because the increase in radiation at the gas inlet may be relevant to the power balance, it could also be advantageous to have bolometers in sectors with gas inlet to monitor the radiated power and produced neutral particles.

For the total radiated power determination a subset of lines of sight may be sufficient. Although an adequate subset can probably be selected from the proposed lines of sight, the best geometry for this subset would be a number of approximately vertical lines of sight complemented by some lines of sight that view into the divertor legs. In the proposed design there were not enough blanket sockets to achieve this, without sacrificing a proper coverage of the upper edge. It would be advantageous to have such lines of sight in another cross-section. These lines of sight could be used for feedback purposes, not requiring a full tomographic reconstruction.

The possibility of toroidal lines of sight has not been discussed. When toroidal symmetry can be assumed these could, in principle, complement ex-divertor views deep into the divertor, or replace blanket bolometers on the high-field side. Technically, however, toroidal views are very hard to accomplish given the curvature of the toroidal gaps between blanket modules. Therefore, such views have not been considered. Toroidal views from the ports alone would not be sufficient to replace blanket bolometers.

### 6.2 Priorities

The considerations in Sec. 4 and the additional views proposed in Sec. 6.1 lead to the priorities given in Table III. Note that the priority views given in the table are the views that carry the most important information. Tomography (without more *a priori* information) will be hard with such

a subset, as the simulations in Sec. 5.3.3. indicate. If the number of channels has to be reduced, it would be preferable to have more views with fewer channels (as the simulation with every second channel indicates).

***Table III*** *Line-of-sight summary and priorities.*

| Purpose | Description | Number of channels |
|---|---|---|
| Priority channels | total | 200 |
| | Ports (divertor, bulk and edge) | 80 |
| | 2 perpendicular divertor fans per leg | 55 |
| | 2 divertor views from blanket | 20 |
| | 5 edge views from blanket | 25 |
| | 2 bulk views from blanket | 20 |
| Detailed tomography | Extra lines of sight in blanket and divertor | 200 |
| Total power | Lines of sight vertical and into divertor legs | 20– 30 |
| Gas inlet monitor | Subset of priority channels in gas inlet sectors | 50…100 |
| Toroidal asymmetries | Subsets ( 15) of priority channels in many sectors | 100…200 |

### 6.3 General conclusions

A detailed design of the lines of sight for bolometry on ITER has been made. The suitability of the proposed lines of sight for tomography has been assessed by phantom simulations. Present-day tomography methods can be used, although with the required large number of grid points the reconstructions are very time and memory consuming. This does not seem to be a problem for ITER, given the continuous improvement of computers. Although the radiation in the divertor can be reconstructed reasonably well (features of the order of 20 cm can be distinguished), and the bulk radiation separately, improvements to the tomography method are required and seem feasible. A prerequisite is that all measurements are in the same poloidal cross-section, or not more than one sector apart. This requires the movement of an instrumental divertor cassette. Subsets of the lines of sight in other toroidal locations can give information on toroidal asymmetries, edge gas inlet effects and the radiated power. The systems can be used for feed-back purposes on the total radiated power, the edge location and the position of the radiating region in the divertor. The divertor measurements can give information on charge-exchange neutral losses that are expected in the divertor. Using fewer lines of sight than proposed has a negative effect on the quality of the tomographic reconstructions, in particular when the number of views is reduced. The fact that fewer lines of sight and views give worse reconstructions and that the bulk reconstructions when using all lines of sight are not particularly good (apart from the total radiation), indicate that in the experimental conditions of ITER the maximum number

of feasible lines of sight is required to have the best chance to reconstruct the emission profiles adequately. In particular, if good reconstructions of the radiation at strike points is required, more divertor lines of sight than used in the current simulations are needed. However, when sufficient experience has been gained it may be possible to work with a reduced set of lines of sight. Using moderately more lines of sight only gives limited improvements. The work described in this report is based on the design of ITER in July 1997. Modifications to the ITER design will require an update of the line of sight proposal, for which this report can serve as a starting point.

## ACKNOWLEDGEMENTS

The provision of relevant ITER data by C. Walker, L. de Kock, S. Gerasimov, D. Bouched, and A.S. Kukushkin is gratefully acknowledged. We also thank L. Horton and A. Loarte for their help with the construction of phantoms.

## REFERENCES

[1] R.Reichle, M. Di Maio, and L.C. Ingesson, “Progress of the reference design for ITER bolometers and development of a high-performance alternative, ” to appear in *Proceedings of ITER diagnostics workshop*, Varenna, 1997

[2] C. Walker and L. de Kock, private communication, December 1997

[3] R.Reichle *et al.*, “Bolometer for ITER,” in *Diagnostics for experimental thermonuclear fusion reactors* (proceedings of workshop in Varenna, 1995), Eds. P.E. Stott *et al.* (Plenum Press, New York, 1996), pp. 559

[4] L. de Kock, Design Description Document, Bolometer System (Core and Divertor),ITER report WBS 5.5.D.01, (1997)

[5] M. Di Maio, R. Reichle, and R. Giannella, “Design of a ferro-electric bolometer,” to appear in *Proceedings of the 17th IEEE/NPSS Symposium on Fusion Engineering*, San Diego, October 1997

[6] M. Di Maio and R. Reichle, “Ferro-electric bolomenter,” UK Patent application, provisional No. 9623239, Nov. 1996

[7] F. Natterer, *The mathematics of computerized tomography* (Teubner, Stuttgart/Wiley, New York, 1986)

[8] R.M. Lewitt, “Reconstruction algorithms: transform methods,” Proc. IEEE **71**, 390 (1983)

[9] Y. Censor, “Finite series-expansion methods,” Proc IEEE **71**, 409 (1983)

[10] R.S. Granetz and P. Smeulders, “X-ray tomography at JET,” Nucl. Fusion **28**, 457 (1988)

[11] L.C. Ingesson and V.V. Pickalov, “An iterative projection-space reconstruction algorithm for tomography systems with irregular coverage,” J. Phys. D: Appl. Phys. **29**, 3009 (1986)

[12] L.C. Ingesson *et al.*, “Soft x-ray tomography during ELMs and impurity injection in JET,” submitted to Nucl. Fusion

[13] J.C. Fuchs *et al.*, "Two-dimensional reconstruction of the radiation power density in ASDEX Upgrade," in *Proceedings of the 21st EPS Conference on Controlled Fusion and Plasma Physics*, Montpellier, 27 June – 1 July 1994, Ed. E. Joffrin, *et al.*, Europhysics Conference Abstracts Vol. 18B (EPS, 1994), Part III, pp. 1308

[14] L.C. Ingesson *et al.*, "Radiation distribution and neutral-particle loss in the JET MkI and MkIIA divertors," in *Proceedings of the 24th EPS Conference on Controlled Fusion and Plasma Physics*, Berchtesgaden, Germany, 9–13 June 1997, Ed. M. Schittenhelm *et al.* (EPS, 1997), Vol. 21A, Part I, pp. 113

[15] M. Anton *et al.*, "X-ray tomography on the TCV tokamak," Plasma Phys. Control. Fusion **38**, 1849 (1996)

[16] G.C. Fehmers *et al, 'A model-independent algorithm for ionospheric tomography 1. Theory and Tests,'* Radio Science **33**, 149(1998)

[17] A.S. Kukushkin *et al.*, "Effect on light impurities on the divertor performance in ITER," in *Proceedings of the 24th EPS Conference on Controlled Fusion and Plasma Physics*, Berchtesgaden, Germany, 9–13 June 1997, Ed. M. Schittenhelm *et al.* (EPS, 1997), Vol. 21A, Part III, pp. 1001

[18] A.S. Kukushkin *et al.*, Proceedings of the 16th IAEA Fusion Energy Conference, Montreal, 1996

[19] D. Bouched, Private communication July 1997

[20] S. Gerasimov, private communication July 1997

[21] R. Reichle *et al.*, "Low energy neutral particle fluxes in the JET divertor," J. Nucl. Mat. **241-243**, 456 (1997)

[22] L.C. Ingesson *et al.*, "Projection-space methods to take into account finite beam-width effects in two-dimensional tomography algorithms," submitted to J. Opt. Soc. Am. A

[23] J. Howard, "Tomography and reliable information," J. Opt. Soc. Am. A **5**, 999 (1988)

[24] Reference 7, pp. 71